ЖЭТФ, 2020, том 158, вып. 2 (8), стр. 295–299

SELF-CONSISTENT MODEL OF EXTRAGALACTIC NEUTRINO FLUX FROM EVOLVING BLAZAR POPULATION

A. Neronov [a,b*], ***D. Semikoz*** [a]

[a] *APC, Université Paris Diderot, CNRS/IN2P3, CEA/IRFU, Observatoire de Paris, Sorbonne Paris Cité 75205, Paris, France*

[b] *Astronomy Department, University of Geneva, Ch. d'Écogia 16 Versoix, 1290, Switzerland*

Received December 20, 2019,
revised version December 20, 2019
Accepted for publication December 25, 2019

DOI: 10.31857/S0044451020080064

The origin of astrophysical neutrino signal [1] detected in "high-energy starting events" (HESE) [2] and muon neutrino [3] channels by IceCube telescope is uncertain. The overall flux and spectral slope of the HESE signal are consistent with the high-energy extrapolation of the gamma-ray flux detected by Fermi telescope up to the TeV band [4–9]. However, the anisotropy pattern of the signal does not reveal strong excess toward the Galactic Plane [10–12]. The neutrino signal at energies higher than several hundred TeV sampled from the Northern hemisphere with muon neutrinos reveals harder spectrum compared to that of the HESE neutrino flux [3, 13]. This hardening could be due to the presence of extragalactic component of the astrophysical neutrino flux. The overall flux of the hard component is at the level consistent with the observed ultra-high-energy cosmic ray (UHECR) flux [14–19].

Radio-loud Active Galactic Nuclei (AGN) are among astronomical source classes in which physical conditions which enable acceleration of protons and nuclei to energies up to UHECR range are realised [20–22]. Neutrino emission from AGN, and in particular from blazars, is widely discussed in the context of hadronic models of AGN activity [20, 21, 23–35]. This neutrino emission is expected to be accompanied by the γ-ray emission produced in result of development of electromagnetic cascade inside the neutrino emitting source. In this respect, it is surprising that brightest and/or nearest gamma-ray blazars do not appear as brightest neutrino sources [36, 37]. The only extragalactic source for which evidence for neutrino signal was found is a blazar TXS $0506+056$ [38, 39]. As it is discussed in Ref. [20] not all blazars are expected to be "neutrino-loud". Differences in overall gamma-ray and neutrino emission power are generically expected because neutrinos are efficiently produced only in the presence of dense matter and radiation backgrounds [20, 21, 23, 24, 29].

We explore constraints on neutrino emitting blazar population imposed by observational properties of the neutrino signal: the absence of event clustering in neutrino arrival directions, a problem first noticed in the analysis of Ref. [40], and the fact that nearby blazars are not strong neutrino sources, with the nearest identified neutrino emitted blazar TXS $0506+056$ at redshift ≈ 0.3 [41] which is by a factor ~ 10 further away than the closest gamma-ray blazar (Mrk 421).

We consider standard candle type sources with luminosity function $\rho(L_E, z)\, dL_E$ (the comoving number density of sources at a given redshift z having spectral luminosities L_E to $L_E + dL_E$ at an energy E) which is proportional to a δ function

$$\rho(L_E, z) = \rho_*(1+z)^{\zeta}\delta(L_E - L_{E*}(E)),$$

where $L_{E*}(E) \propto E^{1-\gamma}$ is assumed to be a powerlaw with the slope γ. We allow the standard candle luminosity to evolve with redshift as $(1+z)^{\zeta}$. Models considered in Monte-Carlo simulations described below assume either positive evolution up to z_* followed by no-evolution period between z_* and $z_{max} = 3$. Such evolution patterns are characteristic for blazar populations: flat spectrum radio quasars (FSRQ) [42] and BL Lacs [43] as well as to the parent populations of

* E-mail: andrii.neronov@gmail.com

FSRQs and BL Lacs, Fanaroff-Riley radio galaxies of type I and II [44, 45] and to X-ray selected AGN [46].

Assuming that neutrino flux is emitted into a jet with an opening angle θ_{jet} one could find that the average number of neutrino events detectable with a telescope with effective collection area A_{eff} within exposure time T_{exp} is related to the luminosity L_E as

$$N_\nu(E_*) = (1+z)^{2-\gamma}\frac{A_{eff}T_{exp}L_E(E_*)}{\pi\theta_{jet}^2 d_L^2}, \qquad (1)$$

where d_L is the luminosity distance. If the jet directions are randomly distributed, the probability to find a given source with a jet pointing in the direction of an observer is $p_{obs} = \theta_{jet}^2/2$ so that the "effective" density of sources visible for an observer is $\rho_{eff}(L_E, z) = \theta_{jet}^2\rho(L_E, z)/2$.

The number of observable sources in the redshift range z to $z + dz$ and producing given number of neutrino events between N_ν and $N_\nu + dN_\nu$ is

$$\eta(N_\nu, z)\, dN_\nu dz = \rho_{eff}(L_E, z)\, dL_E dV_C, \qquad (2)$$

where L_E is expressed through N_ν using Eq. (1), dV_C is the comoving volume element per steradian of the telescope field-of-view $dV_C = d_C^2/(H_0E(z))\, dz$ where

$$E(z) = \sqrt{\Omega_{0,m}(1+z)^3 + \Omega_{0,\Lambda}}$$

with $\Omega_{0,m}, \Omega_{0,\Lambda}$ being the present day dark matter and dark energy density parameters and d_C is the comoving distance.

Calculating L_E from (1) and substituting the expression for the comoving volume element in the right hand side of Eq. (2) and integrating over the redshifts we find the differential source count (the number of sources contributing between N_ν and $N_\nu + dN_\nu$ counts):

$$n(N_\nu) = \int_0^\infty \eta(N_\nu, z)\, dz = \\ = \frac{\pi\theta_{jet}^4}{2H_0A_{eff}T_{exp}}\int_0^\infty \frac{d_L^4\rho(L_E, z)}{(1+z)^{4-\gamma}E(z)}\, dz. \qquad (3)$$

The total number of sources producing at least m events within a given exposure is $\mathcal{N}_s(N_\nu > m) = \int_m^\infty n(N_\nu)\, dN_\nu$.

To properly deal with small m case, we use Monte-Carlo simulations of the signal from a source population. We first generate source distribution which we assume to be uniform throughout the comoving volume. For each source we ascribe a fixed luminosity depending on the source distance/redshift (in this sense, we assume "pure luminosity" evolution model, rather than "luminosity dependent density evolution" model which better suits the description of population of blazars [42, 43]). Fixing the position and luminosity of each source, we calculate its expected relative contribution to the neutrino flux at Earth as a function of (properly redshifted) neutrino energy, assuming that all sources have powerlaw type spectra with the slope $\gamma = 2$. Our calculation takes into account the source position on the sky, and the declination dependence of the IceCube effective area $A_{eff}(E)$ [3,13]. We simulate the neutrino signal with total statistics $N_{\nu,tot} \approx 24$ that corresponds to the published IceCube sample of muon neutrinos [3] with muon energy proxies above 200 TeV, if the residual atmospheric neutrino background (approximately one third of the muon neutrino sample) is removed. We assume that detected muons have experienced an order-of-magnitude energy loss before entering the IceCube detector. We retain only muons which arrive at the detector with energies above 200 TeV.

Non-observation of sources producing multiplet events in IceCube indicates that the effective source density is low enough so that typically there are no sources contained within a sphere of the radius at which an individual source produces one event. Assuming that $z_m \ll 1$ one could find that sources produce on average m events as a distance

$$d_m = \sqrt{A_{eff}T_{exp}L_{E*}/(\pi\theta_{jet}^2 m)}.$$

The condition that there is less than one source within the volume of the sphere with radius d_m is then

$$\rho_{*,eff} \lesssim (3/4\pi)\left(\pi\theta_{jet}^2 m/(A_{eff}T_{exp}L_{E*})\right)^{3/2}$$

imposes an upper bound on a combination $\rho_{*,eff}L_{E*}^{3/2}$ of the source density and luminosity, as discussed in Ref. [40].

This analytical result which neglects the Poisson nature of the signal is confirmed by the Monte-Carlo simulation results shown in Fig. 1. The boundary of the dark grey shaded band follows the $\rho_{*,eff}L_{E*}^{3/2} \sim$ const dependence at large source densities, but deviates from it at low densities, where the sources become sparse and Poisson fluctuations of the signal becomes more important. The x axis on Fig. 1 shows the bolometric luminosity $L = \int_{200\ \mathrm{TeV}/\epsilon}^\infty L_E dE$.

Absence of identified sources at the distances closer than $z = 0.3$ imposes an additional constraint which becomes stronger than the constraint from the absence of doublets at high source densities. Qualitative explanation for this fact is that as the source density

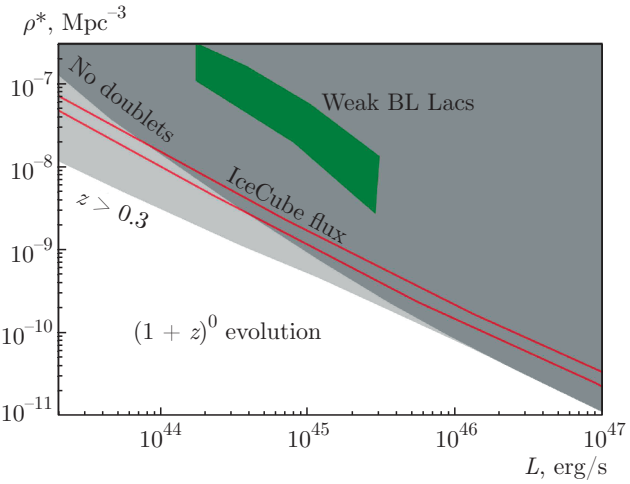

Fig. 1. (Color online) 95 % confidence level constraints on the properties of non-evolving standard candle neutrino source population. Dark grey shading shows constraint from non-observation of doublets in the muon neutrino sample. Light grey shows constraint from non-observation of neutrino-emitting blazars within redshift $z < 0.3$. Red band shows the source density required for production of the observed muon neutrino flux. For comparison, luminosity dependent density of weak BL Lacs from Ref. [43] (green shading) is shown

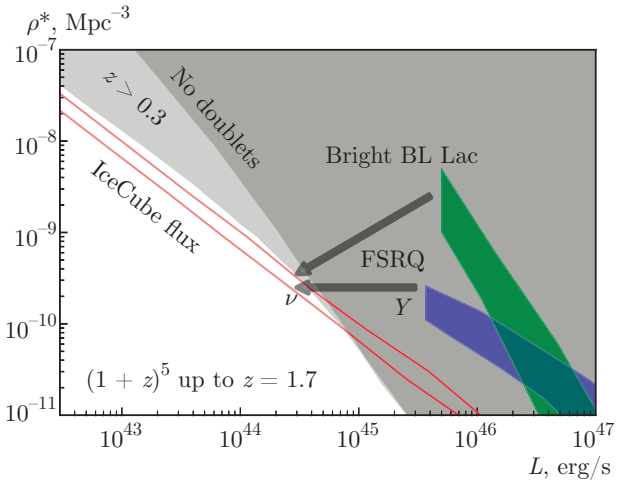

Fig. 2. (Color online) Same as in Fig. 1 but for sources evolving with $\zeta = 5$ up to redshift $z = 1.7$ [46]. For comparison, luminosity dependent densities of FSRQs (blue shading) from Ref. [42] and bright BL Lacs from Ref. [43] are shown

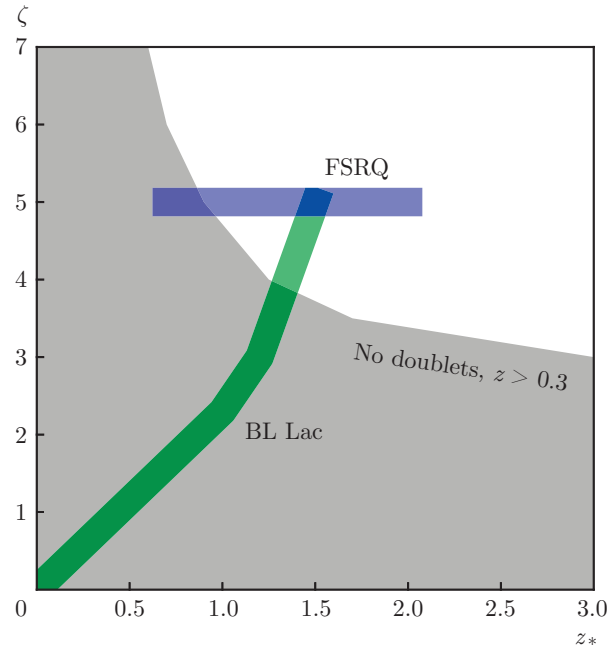

Fig. 3. (Color online) Allowed region of evolution parameters for source populations (white area) compared to the evolution parameters of BL Lac [43] and FSRQ populations [42]

grows, it becomes more and more difficult not to notice very nearby sources (which we assume are all identified as blazars using techniques of multi-wavelength astronomy). Nevertheless, also this constraint shows dependence on the source luminosity because the individual sources get weaker and weak nearby sources on average contribute with less than one neutrino to the signal. The first identifiable source which occasionally produces one event in a given exposure is not necessarily the nearest one.

A combination of the absence of doublets and absence of nearby sources constraints rules out the possibility that the IceCube muon neutrino flux is generated by a population of non-evolving sources, like Low-luminosity BL Lac and Fanaroff-Riley type I (FR I) radio galaxies which show no or negative cosmological evolution [43, 44]. This is clear from comparison of the constraints with the density of the sources required for generation of the observed neutrino flux, shown as the red band in Fig. 1. The red band is never found within the allowed range of ρ_*, L.

The constraints from non-observation of doublets and nearby sources are relaxed if the source population is assumed to evolve positively with the redshift, similarly to high-luminosity BL Lacs and/or FSRQ (and, possibly their progenitors, high luminosity FR II type radio galaxies) [42–45] which evolve as fast as $\zeta = 5$ up to $z_* \sim 1 \ldots 2$.

Figure 2 shows that for fast enough evolution with $\zeta \geq 5$ the combined constraint from non-observation of doublets and nearby sources do not rule out a range of source densities needed to provide the observed IceCube muon neutrino flux. Figure 3 shows the allowed range of evolution parameters z_*, ζ within which source population could explain the IceCube muon neu-

trino flux avoiding constraints from non-identification of nearby sources and absence of doublets in IceCube dataset.

Comparison of the properties of the populations of gamma-ray and neutrino emitting blazars is shown in Figs. 1–3, and where we have overplotted the luminosity function and evolution parameters of BL Lacs from Ref. [43] and FSRQs from Ref. [42]. One could see that sources evolving as weak BL Lacs could not explain the IceCube signal, in spite of the fact that weak BL Lac population avoids the constraint on the absence of correlation of source positions with IceCube neutrinos, as discussed in Ref. [35].

Only the evolution parameters of the highest luminosity BL Lacs ($\zeta > 4$, $z_* > 1.5$) become consistent with IceCube data. Such evolution is valid only for BL Lacs with gamma-ray luminosities in excess of 10^{46}–10^{47} erg/s. The density of those sources is very low, $n \sim 10^{-9}$–10^{-11} Mpc^{-3}.

Figure 3 shows that the evolution parameters bright BL Lacs and FSRQ populations are consistent with constraints on evolution parameters of neutrino sources. From Fig. 2 one could judge that the density of FSRQs and bright BL Lacs is comparable with the density required for neutrino sources evolving as $(1+z)^5$, similarly to the FSRQ and bright BL Lacs. Low-lumnosity FSRQs and/or bright BL Lacs could be considered as viable neutrino source candidates [20, 47], provided that their neutrino luminosity is much lower than γ-ray luminosity. Assumption of comparable γ-ray and neutrino luminosities would violate constraints stemming from the absence of correlations of neutrino arrival directions with γ-ray source positions on the sky [36, 37, 40, 48]. One could also see that neutrino-to-γ-ray luminosity ratio has to be lower for the brightest FSRQs, otherwise they would be individually detectable neutrino sources.

FSRQs are less abundant in the low-redshift Universe than low-luminosity BL Lacs. The closest FSRQ, 3C 273, is at the redshift $z \approx 0.16$ [49]. There are only about 10 FSRQs within the redshift < 0.3 detected by Fermi/LAT [50] and 3C 273 is brightest among them. The neutrino emitting blazar TXS $0506+056$ is classified as BL Lac in SIMBAD astronomical database, but its luminosity scale is closer to that of FSRQs.

TXS $0506+056$ multi-messenger detection could provide a useful insight into neutrino-to-gamma-ray luminosity ratio. Its multi-messenger gamma-ray + neutrino spectrum is shown in Fig. 4. To produce this figure, we have taken the estimate of the time-averaged neutrino flux from the source from Ref. [39] and complemented it with the Fermi/LAT time averaged spectrum which we have extracted from the LAT data collected between 2008 and 2018 (fully covering the IceCube exposure). One could see that the time averaged gamma-ray flux of TXS $0506+056$ is more than an order-of-magnitude higher than the time-averaged neutrino flux.

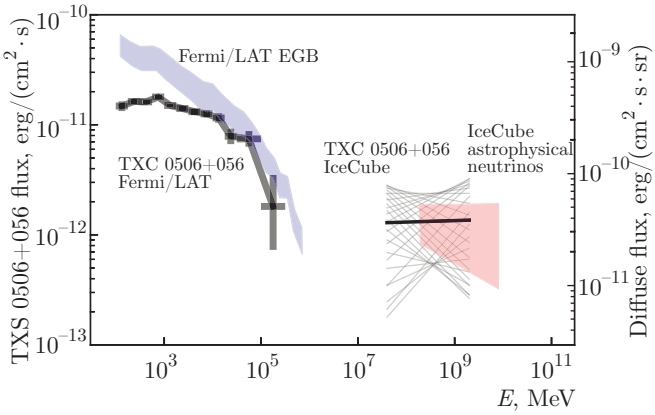

Fig. 4. (Color online) Multi-messenger time-averaged spectrum of TXS $0506+056$ measured by IceCube [39] (butterfly and black horizontal line) and Fermi/LAT (grey data points)

Figure 4 also shows a comparison of the characteristics of the multi-messenger spectrum of TXS $0506+056$ with those of the entire neutrino+gamma-ray extragalactic sky [3, 51]. We have chosen the y axis range in such a way that the TXS $0506+056$ gamma-ray flux does not exceed the extragalactic gamma-ray flux range. With such y-axis range adjustments, it becomes clear that neutrino-to-gamma-ray flux ratio measurements and upper limit for TXS $0506+056$ is consistent with the neutrino-to-gamma-ray flux ratio of entire extragalactic sky.

Overall, we conclude that the hypothesis of the rapidly evolving part of blazar population (bright BL Lacs, FSRQs) contribution to the extragalactic neutrino flux is consistent with the observational data (absence of doublets in IceCube muon neutrino sample and $z \approx 0.3$ redshift of the nearest detected source), once the details of cosmological evolution of the source population and differences in the overall luminosity and anisotropy patterns of gamma-ray and neutrino emission are taken into account.

The full text of this paper is published in the English version of JETP.

REFERENCES

1. IceCube Collab., Science **342**, 6161 (2013).

2. M. G. Aartsen et al., Phys. Rev. Lett. **113**, 101101 (2014).

3. M. G. Aartsen et al., Astrophys. J. **833**, 3 (2016).

4. A. Neronov, M. Kachelrieß, and D. V. Semikoz, Phys. Rev. D **98**, 023004 (2018).

5. A. Neronov and D. Semikoz, Phys. Rev. D **93**, 123002 (2016).

6. A. Neronov and D. Semikoz, Astropart. Phys. **75**, 60 (2016).

7. A. Neronov and D. Semikoz, Astropart. Phys. **72**, 32 (2016).

8. A. Neronov, D. Semikoz, and C. Tchernin, Phys. Rev. D **89**, 103002 (2014).

9. G. Giacinti, M. Kachelrieß, and D. V. Semikoz, JCAP **2018**(7), 051 (2018).

10. M. G. Aartsen et al., Astrophys. J. **849**, 67 (2017).

11. A. Albert et al., arXiv:1808.03531.

12. A. Albert et al., Phys. Rev. D **96**, 062001 (2017).

13. M. G. Aartsen et al., Astrophys. J. **809**, 98 (2015).

14. E. Waxman and J. Bahcall, Phys. Rev. D **59**, 023002 (1999).

15. G. Giacinti, M. Kachelrieß, O. Kalashev, A. Neronov, and D. V. Semikoz, Phys. Rev. D **92**, 083016 (2015).

16. M. Kachelrieß, O. Kalashev, S. Ostapchenko, and D. V. Semikoz, Phys. Rev. D **96**, 083006 (2017).

17. V. S. Beresinsky and G. T. Zatsepin, Phys. Lett. B **28**, 423 (1969).

18. V. S. Berezinskii and A. I. Smirnov, Astrophys. Space Sci. **32**, 461 (1975).

19. X. Rodrigues, A. Fedynitch, S. Gao, D. Boncioli, and W. Winter, Astrophys. J. **854**, 54 (2018).

20. A. Y. Neronov and D. V. Semikoz, Phys. Rev. D **66**, 123003 (2002).

21. A. Neronov, D. Semikoz, and S. Sibiryakov, Month. Not. Roy. Astron. Soc. **391**, 949 (2008).

22. A. Y. Neronov, D. V. Semikoz, and I. I. Tkachev, New J. Phys. **11**, 065015 (2009).

23. K. Mannheim and P. L. Biermann, Astron. Astrophys. **221**, 211 (1989).

24. K. Mannheim, Astron. Astrophys. **269**, 67 (1993).

25. C. Tchernin, J. A. Aguilar, A. Neronov, and T. Montaruli, Astron. Astrophys. **555**, A70 (2013).

26. M. Cerruti, A. Zech, C. Boisson, G. Emery, S. Inoue, and J.-P. Lenain, arXiv:1810.08825.

27. M. Cerruti, A. Zech, C. Boisson, G. Emery, S. Inoue, and J.-P. Lenain, arXiv:1807.04335.

28. R.-Y. Liu, K. Wang, R. Xue, A. M. Taylor, X.-Y. Wang, Z. Li, and H. Yan, arXiv:1807.05113.

29. C. Righi, F. Tavecchio, and S. Inoue, arXiv: 1807.10506.

30. P. Padovani, P. Giommi, E. Resconi, T. Glauch, B. Arsioli, N. Sahakyan, and M. Huber, Month. Not. Roy. Astron. Soc. **480**, 192 (2018).

31. A. Keivani et al., Astrophys. J. **864**, 84 (2018).

32. S. Ansoldi et al., Astrophys. J. Lett. **863**, L10 (2018).

33. K. Murase, F. Oikonomou, and M. Petropoulou, Astrophys. J. **865**, 124 (2018).

34. S. Gao, A. Fedynitch, W. Winter, and M. Pohl, Nature Astron. **3**, 88 (2018).

35. A. Palladino, X. Rodrigues, S. Gao, and W. Winter, arXiv:1806.04769.

36. A. Neronov, D. V. Semikoz, and K. Ptitsyna, Astron. Astrophys. **603**, A135 (2017).

37. M. G. Aartsen et al., Astrophys. J. **835**, 45 (2017).

38. M. Aartsen et al., Science **361**, 1378 (2018).

39. M. Aartsen et al., Science **361**, 147 (2018).

40. K. Murase and E. Waxman, Phys. Rev. D **94**, 103006 (2016).

41. S. Paiano, R. Falomo, A. Treves, and R. Scarpa, Astrophys. J. Lett. **854**, L32 (2018).

42. M. Ajello et al., Astrophys. J. **751**, 108 (2012).

43. M. Ajello et al., Astrophys. J. **780**, 73 (2014).

44. E. M. Sadler et al., Month. Not. Roy. Astron. Soc. **381**, 211 (2007).

45. V. Smolčić et al., Astrophys. J. **696**, 24 (2009).

46. G. Hasinger, T. Miyaji, and M. Schmidt, Astron. Astrophys. **441**, 417 (2005).

47. K. Murase, arXiv:1511.01590.

48. A. Dekker and S. Ando, JCAP **2019**(2), 002 (2019).

49. T. J.-L. Courvoisier, Astron. Astrophys. **9**, 1 (1998).

50. F. Acero et al., Astrophys. J. Supp. **218**, 23 (2015).

51. M. Ackermann et al., Astrophys. J. **799**, 86 (2015).